User-Centric Cross-Tier Base Station Clustering and Cooperation in Heterogeneous Networks: Rate Improvement and Energy Saving

Weili Nie, Fu-Chun Zheng, *Senior Member, IEEE*, Xiaoming Wang, Wenyi Zhang, *Senior Member, IEEE*, and Shi Jin, *Member, IEEE*

***Abstract*—Heterogeneous cellular networks (HetNets) are to be deployed for future wireless communication to meet the ever-increasing mobile traffic demand. However, the dense and random deployment of small cells and their uncoordinated operation raise important concerns about various costs issues, among which notably is energy efficiency. Base station (BS) cooperation is set to play a key role in managing interference in HetNets. In this paper, we consider BS cooperation in the downlink HetNets where BSs from different tiers within the respective cooperative clusters jointly transmit the same data to a typical user, and in particular focus on the optimization of the energy efficiency performance. First, based on a proposed clustering model, we derive the spectral efficiency using tools from stochastic geometry. Furthermore, we formulate a power minimization problem with a minimum spectral efficiency constraint and derive the optimal received signal strength (RSS) thresholds under certain approximation. Building upon these results, we could address the problem of how to design appropriate RSS thresholds, taking into account the tradeoff between spectral efficiency and energy efficiency. Simulations show that the proposed clustering model is more energy-saving than the geometric clustering model, and deploying a multitier HetNet is significantly more energy-saving compared to a macro-only network.**

***Index Terms*—Cooperation, energy savings, HetNets, stochastic geometry, user-centric clustering.**

I. Introduction

IT HAS BEEN reported that information and communication technology (ICT) already contributes around 2% of the global carbon dioxide emission and this is expected to increase rapidly in the future [2]. In addition to the environmental impact, the ICT infrastructure is responsible for about 10% of the world's electric energy consumption, to which the wireless telecommunication industry is the major contributor. Therefore, an energy-efficient cellular network operation is needed more than ever before to reduce both the operational costs and carbon footprint of this industry. Recently, designing green cellular networks has received great attention amongst network operators, regulatory bodies (such as 3GPP and ITU) and green communications research projects (such as EARTH and GreenTouch) [3]–[6].

Generally, macro base stations (BSs) are not designed for providing high data rates but for large coverage ranges. Therefore, due to the explosive growth of mobile data traffic, an increasing portion of the mobile data and voice traffic is expected to be offloaded from the macrocell network onto other low power and low cost small cell networks [7], resulting in heterogeneous cellular networks (HetNets) [8]. HetNets comprise a conventional cellular network overlaid with a diverse set of lower-power BSs or access points (APs), such as picocells, femtocells, WiFi APs and perhaps relays. Heterogeneity is expected to be a key feature of future cellular networks, and an essential means for providing higher end-user throughput as well as expanding its indoor and cell edge coverage. Nevertheless, the deployment of a large number of small cells overlaying the macrocells is not without new technical challenges [9].

BS cooperation, which is described varyingly as coordinated multi-point (CoMP) [10] or network multiple-input multiple-output (MIMO) [11], is an effective technique to manage inter-cell interference and improve spectral efficiency. Specifically, cooperation schemes may range from coordinated scheduling and beamforming (CS/CB) [12] to full joint transmission [13], depending on the employed backhaul architecture, tolerable mobility and complexity, and other constraints. Despite falling short of their initial hype [14], BS cooperation is nonetheless of significant potential and may require a redefinition of the different nodes in the HetNets [15]. This requires new tools for performance prediction and analysis.

A. Related Work and Motivations

Recently, a new general model for wireless node distribution based on stochastic geometry has been proposed [16]–[19] and the authors have developed a tractable and reasonably accurate solution for analyzing important metrics such as signal-to-interference-plus-noise ratio (SINR) coverage, average ergodic rate and rate coverage.

Manuscript received July 14, 2015; revised December 6, 2015; accepted March 10, 2016. Date of publication April 7, 2016; date of current version May 19, 2016. This work was supported by the National Basic Research Program of China (973 Program) under Grant 2012CB316004. The work of F.-C. Zheng was supported by the U.K. Engineering and Physical Sciences Research Council (EPSRC) under Grant EP/K040685/1. The work of S. Jin was supported by the National Natural Science Foundation of China under Grant 61531011. The paper was presented in part at IEEE Globecom 2014 [1].

W. Nie, X. Wang, and S. Jin are with the National Mobile Communications Research Laboratory, Southeast University, Nanjing 210093, China (e-mail: monde.nie@gmail.com; wangxiaoming@seu.edu.cn; jinshi@seu.edu.cn).

F.-C. Zheng is with the School of Systems Engineering, University of Reading, Reading RG6 6AY, U.K. (e-mail: fzheng@ieee.org).

W. Zhang is with the Key Laboratory of Wireless-Optical Communications, Chinese Academy of Sciences, Department of Electronic Engineering and Information Science, University of Science and Technology of China, Hefei 230027, China (e-mail: wenyizha@ustc.edu.cn).

Color versions of one or more of the figures in this paper are available online at http://ieeexplore.ieee.org.

Digital Object Identifier 10.1109/JSAC.2016.2551488

Based on the stochastic geometry framework, a number of works have discussed BS cooperation techniques. [20] investigated outage probability of BS cooperation by large-deviation theory. The BSs are clustered using a regular lattice, whereby BSs in the same cluster mitigate mutual interference by zero-forcing beamforming. [21] analyzed intra-cluster interference coordination for randomly deployed BSs, considering a random clustering process where cluster stations are located according to a random point process and groups of BSs associated with the same cluster coordinate. A model for pair-wise BS cooperation with irregular BS deployment was treated in [22]. Coherent joint-transmission with power-splitting with and without additional dirty paper coding was considered. [23] presented a general model for analyzing non-coherent joint-transmission BS cooperation, and characterized SINR distribution under user-centric clustering and channel dependent scheduling. [24] studied the ergodic capacity of a multicell distributed antenna system (DAS), where remote antenna units are spread within each cell to cooperatively transmit to user terminals. [25] extended the work in [23] towards the multi-tier HetNets and derived coverage probability. The authors in [26] considered the problem of BS cooperation in the downlink HetNets by focusing on the joint-transmission scenario, and derived the coverage probability for the typical user and the worst case user, respectively. However, all the above works have seldom dealt with the energy efficiency problem.

Energy efficiency evaluation and optimization in the HetNets have attracted a lot of research interest recently. For instance, [27] studied energy-efficient precoding for CoMP transmission in two-tier HetNets. In [28], a coordinated energy-efficient transmission design for the heterogeneous multicell multiuser downlink systems was studied. [29] considered the energy-efficient transmit beamforming design and power allocation policies in two-tier HetNets. These works are restricted to a simplified two-tier HetNet scenario consisting of one or a small number of macro BSs and a fixed number of small cells in each macro cell. On the other hand, the authors in [30]–[33] studied the energy efficiency problem in the HetNets based on stochastic geometric model. [30] evaluated the performance of two-tier networks in terms of energy efficiency and fairness of resource allocation. [31] studied the design of energy efficient HetNets through the deployment of sleeping strategies. The authors in [32] studied the separation architecture in the HetNets and demonstrated that it can significantly reduce the overall energy consumption of a cellular network. In [33], the heterogeneity of large-scale user behavior was quantitatively characterized and exploited to study the energy efficiency in the HetNets. Nevertheless, these works have not investigated the energy-efficient BS cooperation techniques in the HetNets.

In this work, we consider the energy efficiency (or energy savings) problem of BS cooperation in the HetNets analytically based on the stochastic geometry framework (especially under different path loss exponents). In particular, we model the location of BSs, both the macrocells and small cells, as independent Poisson point processes (PPPs) with different spatial deployment intensities. Inspired by the threshold-based idea that has been extensively applied in BS cooperation [22]–[26] and contention mitigation [34], we consider non-coherent joint-transmission based on tier-specific received signal strength (RSS) thresholds. By using tools from stochastic geometry, we aim at deriving a tractable result for spectral efficiency. From the perspective of energy efficiency, we mainly focus on two issues: the optimal RSS thresholds of different tiers and the performance gains of the proposed clustering model in the HetNets.

B. Contributions and Organizations

Proposed clustering model: We propose a user-centric clustering model based on tier-specific RSS thresholds. Different from the geometric clustering model applied in our previous work [1] where the cooperative set is only determined by the Euclidean distances between BSs and the typical user (also see [23] and [25]), here in this paper we highlight the impact of fading coefficients on clustering thresholds (i.e. the cooperative region of each tier now is a random shape). Compared to the geometric clustering model, it is shown that the proposed clustering model is more energy-saving. More importantly, we now allow path loss exponents for different tiers to be different, a critical fact that, to our best knowledge, has not been considered extensively in the literature.

Characterization of spectral efficiency: We analytically calculate the spectral efficiency for a typical user located at the center of a cooperative cluster in a K-tier HetNet. Based on the stochastic geometry framework, the expression is reasonably tractable and enjoys a high degree of generality. For instance, the analytical result allows the distribution of fading coefficients to be almost arbitrary while our previous work [1] has an assumption of Rayleigh fading. In addition, the energy efficiency can be readily obtained from the result of the area power consumption and spectral efficiency. From the numerical results, it is of critical importance to design appropriate RSS thresholds, taking into account the trade-off between spectral efficiency and energy efficiency.

Optimal RSS thresholds of tiers: we formulate a power minimization problem under a minimum spectral efficiency constraint and derive an approximate result. Instead of minimizing intra-cluster power consumption [1], here we focus on optimizing the total BS power consumption of the network, which is more important in reality. Numerical results demonstrate the tightness of the approximation. Moreover, the approximate result has a closed form in a few special cases. The optimal RSS thresholds are influenced jointly by multiple system parameters, such as deployment densities, transmit power, circuit power, backhaul power and path loss exponents. Based on the optimal RSS thresholds of tiers, simulations show that the extra deployment of small cells is considerably more energy-saving compared to traditional macro-only networks.

In the remainder of this paper, Section II presents the system model. The spectral efficiency is derived in Section III. In Section IV, we optimize the RSS thresholds for the power minimization problem. Numerical results and discussions are provided in Section V. Finally, Section VI concludes the paper. For comparison and consistency, we follow the denotation system in [17]–[25] (unless stated otherwise).

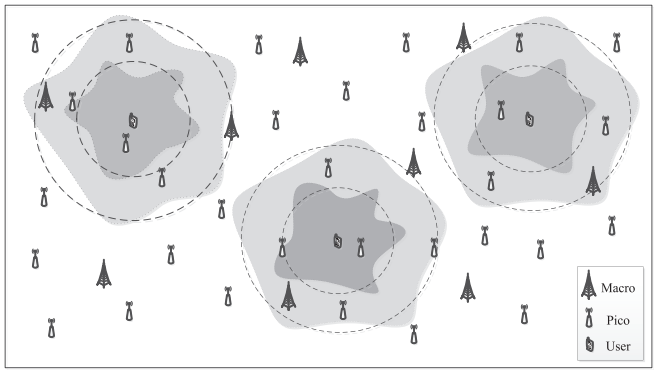

Fig. 1. Illustration of a two-tier HetNet utilizing a mix of macro and pico BSs. Each user is located at the center of its cluster, where the dark region denotes pico tier cooperative region, and the light region denotes macro tier cooperative region. Note that the irregularity of the cooperative region comes from fading coefficients and the dashed circles represent the respective average cooperative regions.

II. System Model

We consider a HetNet composed by K independent network tiers, where each tier is distinguished by its transmit power and deployment density. For example, traditional macro BSs (typically considered as tier 1 and so is it in this work) would usually have a much higher transmit power and lower density (e.g. pico- and femto-cells) [18]. For notational ease, we denote $\mathcal{K} = \{1, 2, \cdots, K\}$. All the network tiers are co-channel deployed. In this work, BSs across tiers differ in terms of deployment density λ_k, transmit power p_k[1], and path loss exponent α_k ($\alpha_k > 2$). The BS locations of each tier are assumed to be realizations from an independent homogeneous PPP $\{\Phi_k\}$. Users are randomly distributed as another independent homogeneous PPP Φ_u with intensity λ_u. BSs and users are all equipped with a single antenna. For the propagation model, we consider the general power-law path loss $l(x) = \|x\|^{-\alpha_k}$, where $\|x\|$ denotes the distance between x and the origin $o \in \mathbb{R}^2$. An example of a two-tier HetNet utilizing a mix of macro and pico BSs is illustrated in Fig. 1, where each user can be served by BS cooperation from different tiers.

A. BS Cooperation Strategy

Without loss of generality, we focus on the downlink analysis for a typical user located at the origin o. For this, the BS cooperation strategy is that a subset of the total ensemble of BSs cooperate by jointly transmitting the same data to the typical user. This kind of BS cooperation strategy is feasible in the "lightly-loaded" scenario [35], i.e. $\lambda_u \ll \sum_{k\in\mathcal{K}} \lambda_k$. As we know, network densification, which is driven by the rise of HetNets, brings about an interesting and novel phenomenon: Each user competes only with a relatively small number of other users for a BS's service and it may even have one or more BSs to solely serve itself [15], [36]. In such a sense, the assumption of "lightly loaded" scenario will be very relevant in future HetNets.

[1]Unless stated otherwise, p_k refers to the transmit power of the BS serving its each user in the k^{th} tier.

Denote by $\mathcal{C}_c \subset \cup_{k=1}^{K} \Phi_k$ the set of the cooperative BSs for the typical user. Consequently, the link from the cooperative BSs to the typical user is a multiple-input single-output (MISO) channel. Assuming non-coherent joint transmission technique [23], [37] and treating interference as noise, the SINR at the typical user is given by

$$\mathrm{SINR} = \frac{\sum\limits_{x\in\mathcal{C}_c} p_{v(x)} \Psi_x \|x\|^{-\alpha_{v(x)}}}{\sum\limits_{x\in\mathcal{C}_I} p_{v(x)} \Psi_x \|x\|^{-\alpha_{v(x)}} + \sigma^2}, \tag{1}$$

where $\mathcal{C}_I \subset \cup_{k=1}^{K} \Phi_k$ denotes the set of the interfering BSs, $v(x)$ returns the index of network tier to which the BS located at $x \in \mathbb{R}^2$ belongs, i.e. $v(x) = k$ iff $x \in \Phi_k$, $p_{v(x)}$ is the transmit power of the BS located at x, Ψ_x denotes the fading coefficient from the BS located at x to the typical user and σ^2 is the white noise power.

B. BS Clustering Model

The clustering method adopted in this work is user-centric, in which each user chooses its surrounding BSs dynamically to form its serving subset. Note that throughout this paper, we slightly abuse notation denoting BS clustering by clustering. Considering the typical user located at the origin, we group BSs with sufficiently high RSS to the typical user into a cooperative cluster. Namely, the i^{th} BS from the k^{th} tier located at $x_{k,i}$ belongs to the cooperative cluster of the typical user only if $p_k \Psi_{x_{k,i}} \|x_{k,i}\|^{-\alpha_k} \geq T_k$, where T_k is the k^{th} tier RSS threshold. Note that here the channel is assumed to be slow-varying (e.g. shadowing) such that the cooperative cluster remains unchanged at least within several data blocks or frames.

In the following, we will substitute $\Psi_{x_{k,i}}$ by $\Psi_{k,i}$ for simplicity, and assume that the fading coefficients $\{\Psi_{k,i}\}_{i=1}^{\infty}$ are i.i.d. random variables with the same distribution as Ψ_k. Furthermore, we allow the distribution of Ψ_k to be arbitrary on the condition that $\mathbb{E}\left[\Psi_k^{2/\alpha_k}\right] < \infty$. Thus, the set of the cooperative BSs from the k^{th} tier for the typical user is

$$\mathcal{C}_{c,k} = \left\{ x_{k,i} \in \Phi_k \,\middle|\, p_k \Psi_{k,i} \|x_{k,i}\|^{-\alpha_k} \geq T_k \right\}. \tag{2}$$

Note that $\mathcal{C}_c = \cup_{k\in\mathcal{K}} \mathcal{C}_{c,k}$ and the threshold T_k serves as a tier-specific and tunable design parameter for optimizing the system performance. Due to the existence of fading coefficients in the clustering model, the cooperative region in each tier turns out to be a random shape and the k^{th} tier mean cooperative radius is given by

$$R_k = \left(\frac{p_k}{T_k}\right)^{\frac{1}{\alpha_k}} \mathbb{E}\left[\Psi_k^{\frac{1}{\alpha_k}}\right]. \tag{3}$$

Furthermore, in order to ensure the effectiveness of the system model, we propose the following assumption.

Assumption 1: Since the locations of all the users are randomly distributed as PPP, the cooperative sets of several different users may overlap. In this case, these users will be assigned to different orthogonal resource blocks.

Note that the overlapping probability is relatively low in a lightly loaded scenario, especially with small cooperative regions[2]. From the above assumption, we can guarantee that there exists no intra-cluster interference, i.e., $\mathcal{C}_I \subseteq \cup_{k=1}^{K} \Phi_k \backslash \mathcal{C}_c$, and all the BSs that are within the cooperative set $\mathcal{C}_c$ will be always available to participate in cooperative transmission.

C. BS Load and Area Power Consumption

Assumption 1 reveals that the BS will accommodate its multiple users with different resource blocks. In a lightly-loaded scenario, however, many BSs have no data to transmit in most of their available resource blocks, and thus the whole network power consumption heavily depends on the number of users that each BS serves.

1) BS Load: We define the BS load as the average number of users that each BS serves simultaneously [19], which, by definition, can be evaluated in the following lemma.

Lemma 1: Let $\mathcal{N}_k$ be the number of users that a BS in the k^{th} tier serves simultaneously on different resource blocks. Then, the BS load in the k^{th} tier is given by $L_k = \mathbb{E}\left[\mathcal{N}_k\right] = \pi \lambda_u \left(\frac{p_k}{T_k}\right)^{2/\alpha_k} \mathbb{E}\left[\Psi_k^{2/\alpha_k}\right]$.

Proof: See Appendix A. ■

We can observe from Lemma 1 that the BS load depends on the user density and RSS thresholds, and by reasonably adjusting the RSS thresholds $\{T_k\}$, the load balancing among different tiers could be achieved.

2) Area Power Consumption: We define the area power consumption as the average consumed BS power per unit area in the HetNets [31], which is given by

$$P_{area} = \sum_{k=1}^{K} \lambda_k P_{in,k}, \tag{4}$$

where $P_{in,k}$ denotes the power consumption per BS in the k^{th} tier. First, we use the linear approximation of the BS power model for each tier [39], [40]. In order to capture the backhauling energy [41] and BS load [40], we extend the linear model to a general form as follows,

$$P_{in,k} = L_k(P_{c,k} + \Delta_k p_k + P_{bh,k}) + P_{0,k}, \tag{5}$$

where $P_{c,k}$ accounts for the dynamic circuit power due to signal processing which is proportional to L_k, Δ_k denotes the slope of the k^{th} tier BS power consumption, $P_{bh,k}$ is the backhauling power per unit load[3], and $P_{0,k}$ is the static circuit power, which is independent of both L_k and p_k. Note that all power parameters we mentioned above are tier-specific. By substituting (5) into (4), we have

$$P_{area} = \sum_{k=1}^{K} \lambda_k P_{0,k} + \lambda_u \sum_{k=1}^{K} \pi \lambda_k \left(\frac{p_k}{T_k}\right)^{\frac{2}{\alpha_k}} \mathbb{E}\left[\Psi_k^{\frac{2}{\alpha_k}}\right] \times \left(P_{c,k} + \Delta_k p_k + P_{bh,k}\right), \tag{6}$$

[2]The overlapping probability could be approximately calculated as $\mathbb{P}_o \approx 1 - e^{-4\pi\lambda_u R_{\max}^2}$, where $R_{\max} = \max_{k\in\mathcal{K}} R_k$ and R_k is given by (3).

[3]The physical meaning of $L_k P_{bh,k}$ can be explained as follows: When the k^{th} tier BS simultaneously receives L_k users' service request, it will be engaged in L_k cooperative clusters according to Assumption 1, which consumes $L_k P_{bh,k}$ of the backhauling power.

where the first term only depends on the BS intensities, the second term not only depends on the BS intensities, but also on the user intensity and cooperative region. Note that the area power consumption also reflects the total BS power consumption of the network.

III. Spectral Efficiency

In this section, we derive the general result of the spectral efficiency at the typical user in the K-tier HetNet. Assume that appropriate adaptive modulation/coding is used, and thus the spectral efficiency (in nats/s/Hz) is

$$\tau = \mathbb{E}_{\text{SINR}}\left[\ln\left(1 + \text{SINR}\right)\right]. \tag{7}$$

The expectation is both spatial and temporal averaging since the SINR of the typical user incorporates the impact of the point processes and the fading coefficients. Note that in a lightly-loaded scenario, the effect of BS load on the user rate is of subordinate importance and thus the spectral efficiency τ could serve as an appropriate performance metric [23].

By substituting (1) into (7), the SINR at the typical user under the proposed clustering model can be obtained, and (7) can be accordingly written as

$$\tau = \mathbb{E}\left[\ln\left(1 + \frac{\sum_{k\in\mathcal{K}} \sum_{x_{k,i}\in\mathcal{C}_{c,k}} p_k \Psi_{k,i} \left\| x_{k,i} \right\|^{-\alpha_k}}{\sum_{k\in\mathcal{K}} \sum_{x_{k,j}\in\mathcal{C}_{I,k}} p_k \Psi_{k,j} \left\| x_{k,j} \right\|^{-\alpha_k} + \sigma^2}\right)\right], \tag{8}$$

where $\mathcal{C}_{I,k} \subseteq \Phi_k \backslash \mathcal{C}_{c,k}$ denotes the set of interfering BSs in the k^{th} tier. The expectation is taken over both the PPP $\{\Phi_k\}$ and fading coefficients $\{\Psi_{k,i}\}$. Note that, for analytical tractability and as in [23] and [26], we consider the worst-case interference strength for the typical user, i.e., all the BSs outside the cooperative cluster $\mathcal{C}_c$ serve as interfering sources (while in reality some of them may not be transmitting, hence our assumption is a "worst-case" scenario), then we have $\mathcal{C}_{I,k} = \Phi_k \backslash \mathcal{C}_{c,k}$. Since we consider a lightly-loaded scenario, this assumption may overestimate the actual interference [23].

The general result of spectral efficiency is evaluated in the following theorem, reflecting the impact of thermal noise as well as per-tier BS density λ_k, transmit power p_k, path loss exponent α_k, RSS threshold T_k and fading coefficient Ψ_k with an arbitrary distribution.

Theorem 1: The spectral efficiency of the typical user in a K-tier HetNet with the proposed BS cooperation strategy and clustering model is given by

$$\tau = \int_0^{\infty} \left\{ \exp\left[-\sum_{k=1}^{K} \pi \lambda_k \mathbb{E}\left[\Psi_k^{\frac{2}{\alpha_k}}\right] (t\, p_k)^{\frac{2}{\alpha_k}} \mathcal{Z}\left(t, T_k, \alpha_k\right) \right] - \exp\left[-\sum_{k=1}^{K} \pi \lambda_k \mathbb{E}\left[\Psi_k^{\frac{2}{\alpha_k}}\right] (t\, p_k)^{\frac{2}{\alpha_k}} \Gamma\left(1 - \frac{2}{\alpha_k}\right) \right] \right\} \frac{e^{-\sigma^2 t}}{t} dt, \tag{9}$$

where $\Gamma(\cdot)$ denotes the gamma function and

$$\mathcal{Z}(t, T_k, \alpha_k) = \gamma\left(1 - \frac{2}{\alpha_k}, T_k t\right) + \left(e^{-T_k t} - 1\right)(T_k t)^{-\frac{2}{\alpha_k}}. \tag{10}$$

Proof: Introduce two auxiliary variables J_S and J_I, which denote the received signal power from the cooperative BSs and the aggregate interference created by interfering BSs, respectively, i.e.,

$$J_S = \sum_{k\in\mathcal{K}} \sum_{x_{k,i}\in\mathcal{C}_{c,k}} p_k \Psi_{k,i} \left\| x_{k,i} \right\|^{-\alpha_k},$$
$$J_I = \sum_{k\in\mathcal{K}} \sum_{x_{k,j}\in\mathcal{C}_{I,k}} p_k \Psi_{k,j} \left\| x_{k,j} \right\|^{-\alpha_k}, \tag{11}$$

where $\mathcal{C}_{c,k}$ is from (2) and $\mathcal{C}_{I,k} = \Phi_k \backslash \mathcal{C}_{c,k}$ since we consider the worst case. Accordingly, (8) can be rewritten as

$$\tau = \mathbb{E}_{J_S, J_I}\left[\ln\left(1 + \frac{J_S}{J_I + \sigma^2}\right)\right]. \tag{12}$$

In order to evaluate the spectral efficiency τ in (12), we first introduce the following useful equation according to [42, Lemma 1],

$$\ln(1 + x) = \int_0^\infty \frac{1}{z}\left(1 - e^{-xz}\right) e^{-z} dz, \tag{13}$$

where $x > 0$. By applying (13) in (12), we have

$$\tau = \mathrm{E}_{J_S, J_I}\left\{\int_0^\infty \frac{e^{-z}}{z}\left[1 - \exp\left(\frac{-z J_S}{J_I + \sigma^2}\right)\right] dz\right\}$$
$$\overset{(a)}{=} \mathrm{E}_{J_S, J_I}\left\{\int_0^\infty \frac{e^{-\sigma^2 t}}{t} \exp(-t J_I)\left[1 - \exp(-t J_S)\right] dt\right\}, \tag{14}$$

where (a) follows from a change of variable $z = t\left(J_I + \sigma^2\right)$. Since J_S and J_I are mutually independent due to $\mathcal{C}_s \cap \mathcal{C}_I = \emptyset$, by applying the Fubini's theorem, we have

$$\tau = \int_0^\infty \frac{e^{-\sigma^2 t}}{t} \mathcal{L}_{J_I}(t)\left[1 - \mathcal{L}_{J_S}(t)\right] dt, \tag{15}$$

where $\mathcal{L}_{J_S}(t)$ and $\mathcal{L}_{J_I}(t)$ are the Laplace transforms of random variables J_S and J_I, respectively. First, using the definition of the Laplace transform yields,

$$L_{J_I}(t) = \mathbb{E}_{J_I}\left[\exp(-t J_I)\right]$$
$$= \mathbb{E}_{\{\Phi_k\},\{\Psi_{k,j}\}}\left[\exp\left(-t \sum_{k\in\mathcal{K}} \sum_{x_{k,j}\in\mathcal{C}_{I,k}} p_k \Psi_{k,j} \left\| x_{k,j} \right\|^{-\alpha_k}\right)\right]$$
$$\overset{(a)}{=} \prod_{k=1}^{K} \mathbb{E}_{\Phi_k,\{\Psi_{k,j}\}}\left[\prod_{x_{k,j}\in\mathcal{C}_{I,k}} \exp\left(-t\, p_k \Psi_{k,j} \left\| x_{k,j} \right\|^{-\alpha_k}\right)\right]$$
$$\overset{(b)}{=} \prod_{k=1}^{K} \exp\left\{-2\pi\lambda_k \mathbb{E}_{\Psi_k}\left[\int_{b_k}^\infty \left(1 - e^{-t\, p_k \Psi_k r^{-\alpha_k}}\right) r dr\right]\right\}, \tag{16}$$

where (a) follows from the independence property of different fading coefficients and BS point processes among tiers, (b) follows from the PGFL of PPP [43] with $b_k = (p_k \Psi_k / T_k)^{1/\alpha_k}$ and we swap the order of integration and expectation according to Fubini's theorem.

By applying a change of variable $u = (t\, p_k \Psi_k)^{-2/\alpha_k} r^2$, (16) can be further simplified as

$$\mathcal{L}_{J_I}(t) = \exp\left[-\sum_{k=1}^{K} \pi\lambda_k (t\, p_k)^{\frac{2}{\alpha_k}} \mathbb{E}\left[\Psi_k^{\frac{2}{\alpha_k}}\right] \mathcal{Z}(t, T_k, \alpha_k)\right], \tag{17}$$

with the definition

$$\mathcal{Z}(t, T_k, \alpha_k) \triangleq \int_{(T_k t)^{-\frac{2}{\alpha_k}}}^\infty \left[1 - \exp\left(-u^{-\frac{\alpha_k}{2}}\right)\right] du. \tag{18}$$

We can calculate the above integral by making a change of variable $v = u^{-\frac{\alpha_k}{2}}$, that is

$$\mathcal{Z}(t, T_k, \alpha_k) = \frac{2}{\alpha_k} \int_0^{T_k t} \left(1 - e^{-v}\right) v^{-\frac{2}{\alpha_k} - 1} dv$$
$$\overset{(a)}{=} \gamma\left(1 - \frac{2}{\alpha_k}, T_k t\right) + \left(e^{-T_k t} - 1\right)(T_k t)^{-\frac{2}{\alpha_k}}, \tag{19}$$

where $\gamma(s, z) = \int_0^z t^{s-1} e^{-t} dt$ is the lower incomplete gamma function, and (a) follows from integration by parts. Combining (16) with (19) completes the calculation of $\mathcal{L}_{J_I}(t)$. Similarly, the expression of $\mathcal{L}_{J_S}(t)$ is given by

$$\mathcal{L}_{J_S}(t) = \exp\left[-\sum_{k=1}^{K} \pi\lambda_k \mathbb{E}\left[\Psi_k^{\frac{2}{\alpha_k}}\right] (t\, p_k)^{\frac{2}{\alpha_k}} \mathcal{Z}'(t, T_k, \alpha_k)\right], \tag{20}$$

where $\mathcal{Z}'(t, T_k, \alpha_k) = \Gamma\left(1 - \frac{2}{\alpha_k}\right) - \mathcal{Z}(t, T_k, \alpha_k)$.

Then by substituting the expressions of $\mathcal{L}_{J_S}(t)$ and $\mathcal{L}_{J_I}(t)$ into (15), we obtain the desired result in (9). ■

Although not a closed form, this expression is amenable to efficient numerical evaluation, as opposed to the usual Monte Carlo methods that rely on repeated random sampling to estimate the results.

Since the network energy efficiency η_{ee} is defined as a ratio of area spectral efficiency η_{ase} to area power consumption P_{area} [31], it can be calculated as

$$\eta_{ee} \triangleq \frac{\eta_{ase}}{P_{area}} = \frac{\lambda_u \tau}{P_{area}}, \tag{21}$$

where the unit is nats/Joule/Hz and P_{area} is from (6).

Remark 1: Note that since $\mathcal{Z}(t, T_k, \alpha_k)$ in (9) increases with T_k, τ is a strictly monotonically decreasing function of $\{T_k\}$. However, the RSS thresholds $\{T_k\}$ cannot be arbitrarily small due to the fact that the area power consumption and BS load would be unrealistically large according to (6) and Lemma 1. Thus, there exists a tradeoff between spectral efficiency and energy saving (or BS load).

IV. Power Minimization Problem

Based on the analytical result of spectral efficiency in Theorem 1, in this section, we want to determine the optimal RSS thresholds in the K-tier HetNet, which minimize the area power consumption in (6) while satisfying the minimum spectral efficiency requirement. Since the BS density is typically large in HetNets, we ignore the noise and focus on the interference-limited regime. Hence, by combining (6) with (9), we formulate the problem as follows,

$$\begin{aligned}\min_{\{T_k\}} \ & \lambda_u \sum_{k=1}^{K} \pi \lambda_k \left(\frac{p_k}{T_k}\right)^{\frac{2}{\alpha_k}} \mathbb{E}\left[\Psi_k^{\frac{2}{\alpha_k}}\right] \left(P_{c,k} + \Delta_k p_k + P_{bh,k}\right) \\ \text{s.t.} \ & \int_0^{\infty} \frac{1}{t} \left\{ \exp\left[-\sum_{k=1}^{K} \pi \lambda_k \mathbb{E}\left[\Psi_k^{\frac{2}{\alpha_k}}\right] (t p_k)^{\frac{2}{\alpha_k}} \mathcal{Z}(t, T_k, \alpha_k) \right] \right. \\ & \left. - \exp\left[-\sum_{k=1}^{K} \pi \lambda_k \mathbb{E}\left[\Psi_k^{\frac{2}{\alpha_k}}\right] (t p_k)^{\frac{2}{\alpha_k}} \Gamma\left(1 - \frac{2}{\alpha_k}\right) \right] \right\} dt \\ & \geq \tau_0 \end{aligned} \tag{22}$$

where the first term of P_{area} in (6) has been omitted due to its independence of $\{T_k\}$, and τ_0 denotes the minimum spectral efficiency, which explicitly characterizes the average QoS requirement of each user.

Note that problem (22) is an optimization problem with K variables and a complicated inequality constraint. In addition, this problem can be implicitly expressed as $\min_{T_K, \mathbb{T}_{-K}} f(T_K, \mathbb{T}_{-K})$, where $\mathbb{T}_{-K} \triangleq \left[T_1, T_2, \cdots, T_{K-1}\right]$ and we define $f(T_K, \mathbb{T}_{-K})$ as the objective function of the problem (21) with the domain restricted to the feasible set, i.e. dom $f = \{(T_K, \mathbb{T}_{-K}) \,|\, g(T_K, \mathbb{T}_{-K}) \geq \tau_0\}$ where $g(T_K, \mathbb{T}_{-K})$ is the expression of average spectral efficiency in Theorem 1. According to [46, Ch4.1.3], for a minimization problem $\min_{T_K, \mathbb{T}_{-K}} f(T_K, \mathbb{T}_{-K})$, if we have $\tilde{f}(\mathbb{T}_{-K}) = \min_{T_K} f(T_K, \mathbb{T}_{-K})$, then the original problem is equivalent to $\min_{\mathbb{T}_{-K}} \tilde{f}(\mathbb{T}_{-K})$. As a result, in the following, we divide problem (22) into two sub-problems to solve it.

A. The First Sub-problem

Suppose that the first $K-1$ tiers' RSS thresholds $\mathbb{T}_{-K}$ are given, the objective function of problem (22) is a strictly monotonically decreasing function of T_K. As a result, problem (22) can be transformed into a sub-problem with a single variable as follows,

$$\begin{aligned}\max_{T_K} \ & T_K \\ \text{s.t.} \ & \int_0^{\infty} \left\{ \exp\left[-\sum_{k=1}^{K} \pi \lambda_k \mathbb{E}\left[\Psi_k^{\frac{2}{\alpha_k}}\right] (t p_k)^{\frac{2}{\alpha_k}} \mathcal{Z}(t, T_k, \alpha_k) \right] \right. \\ & \left. - \exp\left[-\sum_{k=1}^{K} \pi \lambda_k \mathbb{E}\left[\Psi_k^{\frac{2}{\alpha_k}}\right] (t p_k)^{\frac{2}{\alpha_k}} \Gamma\left(1 - \frac{2}{\alpha_k}\right) \right] \right\} \frac{dt}{t} \\ & \geq \tau_0 \end{aligned} \tag{23}$$

Problem (23) has a unique solution, since the left side of the constraint is a strictly monotonically decreasing function of T_K. Instead of obtaining the optimal result numerically through the binary search algorithm, we resort to an analytically tractable lower bound, which will further be shown to be tight through numerical study in Section V.

Theorem 2: Given the first $K-1$ tiers' RSS thresholds $\mathbb{T}_{-K}$, the optimal K^{th} tier RSS threshold has a lower bound T_K^d, which satisfies

$$T_K^d = \left(D_l e^{\frac{\alpha_l - 2}{2} C + \Theta_l - \tau_0} - \sum_{k=1}^{K-1} B_k T_k^{\frac{\alpha_k - 2}{\alpha_k}} \right)^{\frac{\alpha_K}{\alpha_K - 2}}, \tag{24}$$

where C is Euler's Constant, $l \in \mathcal{K}$ and

$$D_l = \frac{(\alpha_K - 2)\, \Gamma\left(1 - \frac{2}{\alpha_K}\right) \omega_l^{\frac{\alpha_l}{2}}}{2\omega_K}, \tag{25}$$

$$B_k = \frac{(\alpha_K - 2)\, \Gamma\left(1 - \frac{2}{\alpha_K}\right) \omega_k}{(\alpha_k - 2)\, \Gamma\left(1 - \frac{2}{\alpha_k}\right) \omega_K}, \ k \in \mathcal{K}, \tag{26}$$

$$\Theta_l = \int_0^{\infty} \frac{\exp\left(-\omega_l t^{\frac{2}{\alpha_l}}\right)}{t} \left[1 - \exp\left(-\sum_{k=1, k \neq l}^{K} \omega_k t^{\frac{2}{\alpha_k}} \right) \right] dt, \tag{27}$$

$$\omega_k = \pi \lambda_k \mathbb{E}\left[\Psi_k^{\frac{2}{\alpha_k}}\right] p_k^{\frac{2}{\alpha_k}} \Gamma\left(1 - \frac{2}{\alpha_k}\right), \ k \in \mathcal{K}. \tag{28}$$

Proof: See Appendix B. ■

Note that the selection of l is arbitrary since (24) takes the same value for any $l \in \mathcal{K}$. Besides, theorem 2 also sheds light on the optimal RSS threshold design when adding a new tier to an existing HetNet.

Remark 2: Fixing per-tier BS density λ_k, the lower bound of T_K is an decreasing function of $T_k, k = 1, 2, \cdots, K-1$. It confirms our intuition that when per-tier BS density is given and the first $K-1$ tiers' cooperative regions decrease, the K^{th} tier cooperative region should be expanded by decreasing the value of T_K.

In addition, the lower bound of T_K is also an decreasing function of τ_0, yielding the following upper bound of the minimum spectral efficiency.

Proposition 1: Given the first $K-1$ tiers' RSS thresholds $\mathbb{T}_{-K}$, the minimum spectral efficiency τ_0 has the maximum value τ_0^{max} that satisfies

$$\tau_0^{\max} = \frac{\alpha_l - 2}{2} C + \Theta_l - \ln \frac{\sum_{k=1}^{K-1} B_k T_k^{\frac{\alpha_k - 2}{\alpha_k}}}{D_l}. \tag{29}$$

Proof: From (24), when $D_l e^{\frac{\alpha_l - 2}{2} C + \Theta_l - \tau_0} - \sum_{k=1}^{K-1} B_k T_k^{\frac{\alpha_k - 2}{\alpha_k}} \geq 0$, a lower bound T_K^d exists. Solving this inequality gives the upper bound of τ_0. ■

The above proposition indicates that when the first tiers' $K-1$ cooperative regions are fixed, even if the K^{th} tier RSS threshold tends towards zero (i.e., the K^{th} tier cooperative

region expands unboundedly), a spectral efficiency $\tau_0 > \tau_0^{\max}$ cannot be achieved.

In the following, we consider two special cases where we can obtain closed-form (approximate) results of Θ_l and T_K^d.

1) Special Case I (Two-tier HetNet): If we consider a two-tier HetNet, i.e., $K = 2$, Θ_l can be rewritten as

$$\Theta_l = \int_0^\infty \frac{\exp\left(-\omega_l t^{\frac{2}{\alpha_l}}\right)}{t}\left[1 - \exp\left(-\omega_j t^{\frac{2}{\alpha_j}}\right)\right]dt, \quad (30)$$

where $j \neq l$ and $j, l \in \{1, 2\}$.

Then we can transform (30) into a series with infinite number of terms, by applying the Taylor series expansion, as follows,

$$\begin{aligned}\Theta_l &= \int_0^\infty \frac{\exp\left(-\omega_l t^{\frac{2}{\alpha_l}}\right)}{t}\left[1 - \sum_{n=0}^{\infty}\frac{(-1)^n \omega_j^n t^{\frac{2n}{\alpha_j}}}{n!}\right]dt \\ &= \int_0^\infty \exp\left(-\omega_l t^{\frac{2}{\alpha_l}}\right)\sum_{n=1}^{\infty}\frac{(-1)^{n+1}\omega_j^n}{n!} t^{\frac{2n}{\alpha_j}-1} dt \\ &\overset{(a)}{=} \sum_{n=1}^{\infty}\frac{(-1)^{n+1}\omega_j^n}{n!}\int_0^\infty t^{\frac{2n}{\alpha_j}-1}\exp\left(-\omega_l t^{\frac{2}{\alpha_l}}\right)dt \\ &\overset{(b)}{=} \frac{\alpha_l}{2}\sum_{n=1}^{\infty}\frac{(-1)^{n+1}}{n!}\left(\omega_j \omega_l^{-\frac{\alpha_l}{\alpha_j}}\right)^n \Gamma\left(\frac{\alpha_l n}{\alpha_j}\right). \end{aligned} \quad (31)$$

where (a) follows from swapping the order of integration and summation according to Fubini's theorem, and (b) follows from a change of variable $x = \omega_l t^{\frac{2}{\alpha_l}}$.

Since the indexes l and j are interchangeable, we can let $l = 2$ if $\omega_1 \omega_2^{-\frac{\alpha_2}{\alpha_1}} < 1$, and $l = 1$ otherwise. Thus the relation between $\omega_1 \omega_2^{-\frac{\alpha_2}{\alpha_1}}$ and 1 makes no difference. Without loss of generality, we focus on the case where system parameters satisfy $\omega_1 \omega_2^{-\frac{\alpha_2}{\alpha_1}} < 1$. Consequently, we only need to take the first M terms to approximate the value of Θ_2, which is

$$\Theta_2 \approx \frac{\alpha_2}{2}\sum_{n=1}^{M}\frac{(-1)^{n+1}}{n!}\left(\omega_1 \omega_2^{-\frac{\alpha_2}{\alpha_1}}\right)^n \Gamma\left(\frac{\alpha_2 n}{\alpha_1}\right) \quad (32)$$

By substituting (32) into (24), we can get a closed-form approximate result T_2^a, which satisfies the following expression:

$$T_2^a = \left(D_2 e^{\frac{\alpha_2 - 2}{2}C + \Theta_2 - \tau_0} - B_1 T_1^{\frac{\alpha_1 - 2}{\alpha_1}}\right)^{\frac{\alpha_2}{\alpha_2 - 2}}. \quad (33)$$

The accuracy of this approximate result will be verified in Section V.

2) Special Case II (Equal Path Loss Exponent): When the path loss exponents of all the tiers are identical, i.e., $\{\alpha_k\} = \alpha$, Θ_l can be rewritten as

$$\begin{aligned}\Theta_l &= \int_0^\infty \frac{\exp\left(-\omega_l t^{\frac{2}{\alpha}}\right)}{t}\left[1 - \exp\left(-t^{\frac{2}{\alpha}}\sum_{k=1, j\neq l}^{K}\omega_k\right)\right]dt \\ &\overset{(a)}{=} \frac{\alpha}{2}\ln\left(\frac{1}{\omega_l}\sum_{k=1}^{K}\omega_k\right), \end{aligned} \quad (34)$$

where (a) follows from (13) with a change of variable $z = \omega_l t^{2/\alpha}$ and ω_k is defined in (28) with $\alpha_k = \alpha$.

By substituting (34) into (24), we have

$$T_K^d = \left(\Xi e^{\frac{\alpha-2}{2}C - \tau_0} - \sum_{k=1}^{K-1}\frac{\omega_k T_k^{\frac{\alpha-2}{\alpha}}}{\omega_K}\right)^{\frac{\alpha}{\alpha-2}}, \quad (35)$$

where

$$\Xi = \frac{(\alpha - 2)\,\Gamma\left(1 - \frac{2}{\alpha}\right)\left(\sum_{k=1}^{K}\omega_k\right)^{\frac{\alpha}{2}}}{2\omega_K}. \quad (36)$$

From the closed-form result in (35), we can obtain an insight in the impact of the K^{th} tier deployment intensity on the K^{th} tier RSS threshold, which is given in the following proposition.

Proposition 2: In the case of equal path loss exponent, given the first $K-1$ tiers' RSS thresholds and deployment intensities, when $\lambda_K \geq \mathcal{G}_1$, T_K^d increases with λ_K, and when $\lambda_K \leq (\mathcal{G}_1 - \mathcal{G}_2)^+$, T_K^d decreases with λ_K, where $(x)^+ = \begin{cases} x, & x > 0 \\ 0, & x \leq 0 \end{cases}$ and $\mathcal{G}_1$, $\mathcal{G}_2$ are given by

$$\mathcal{G}_1 = \frac{2\sum_{k=1}^{K}\mathbb{E}\left[\Psi_k^{\frac{2}{\alpha}}\right]p_k^{\frac{2}{\alpha}}\lambda_k}{(\alpha - 2)\,\mathbb{E}\left[\Psi_K^{\frac{2}{\alpha}}\right]p_K^{\frac{2}{\alpha}}}, \quad (37)$$

$$\mathcal{G}_2 = \frac{4\sum_{k=1}^{K}\mathbb{E}\left[\Psi_k^{\frac{2}{\alpha}}\right]p_k^{\frac{2}{\alpha}}T_k^{\frac{\alpha-2}{\alpha}}\lambda_k}{(\alpha-2)^2\Gamma\left(1-\frac{2}{\alpha}\right)e^{\frac{\alpha-2}{2}C-\tau_0}\left(\sum_{k=1}^{K-1}\omega_k\right)^{\frac{\alpha-2}{2}}\mathbb{E}\left[\Psi_K^{\frac{2}{\alpha}}\right]p_K^{\frac{2}{\alpha}}}. \quad (38)$$

Proof: See Appendix C. ■

Note that Proposition 2 reveals an interesting phenomenon: When the K^{th} tier deployment intensity is sufficiently large to ensure $\lambda_K \geq \mathcal{G}_1$, increasing λ_K leads to a smaller K^{th} tier cooperative region, thus the BS load in the K^{th} tier decreases with λ_K; on the other hand, when the K^{th} tier deployment intensity is sufficiently small to ensure $\lambda_K < (\mathcal{G}_1 - \mathcal{G}_2)^+$, increasing λ_K leads to a larger K^{th} tier cooperative region, thus the BS load in the K^{th} tier increases with λ_K.

Remark 3: In the case of equal path loss exponent, when considering the optimal RSS threshold design of a new network tier adding to the existing HetNet, we can take two possible schemes to reduce the BS load in the new tier: Trying to deploy as few BSs in the new tier as possible or trying to deploy as many BSs in the new tier as possible.

B. The Second Sub-Problem

According to Theorem 2, by substituting (24) into the objective function of the problem (22) and applying some algebraic manipulations, we can formulate the second sub-problem (39) as

$$\begin{aligned}\min_{\mathbb{T}_{-K}} \ & \sum_{k=1}^{K-1} B_k \frac{\alpha_k-2}{\alpha_K-2}\frac{P_{c,k}+\Delta_k p_k+P_{bh,k}}{P_{c,K}+\Delta_K p_K+P_{bh,K}} T_k^{-\frac{2}{\alpha_k}} \\ & + \left(D_l e^{\frac{\alpha_l-2}{2}C+\Theta_l-\tau_0} - \sum_{k=1}^{K-1} B_k T_k^{\frac{\alpha_k-2}{\alpha_k}} \right)^{\frac{2}{2-\alpha_K}} \\ \text{s.t. } & D_l e^{\frac{\alpha_l-2}{2}C+\Theta_l-\tau_0} - \sum_{k=1}^{K-1} B_k T_k^{\frac{\alpha_k-2}{\alpha_k}} \geq 0 \end{aligned} \tag{39}$$

where the constraint exists because only when $D_l e^{\frac{\alpha_l-2}{2}C+\Theta_l-\tau_0} - \sum_{k=1}^{K-1} B_k T_k^{\frac{\alpha_k-2}{\alpha_k}} \geq 0$ can we obtain a feasible value of T_K^d.

A general approximated result of the optimal RSS thresholds $\{T_k^*\}$ is given as follows[4].

Theorem 3: In order to minimize the area power consumption while satisfying the minimum spectral efficiency requirement τ_0, the approximated results of the optimal K tiers' RSS thresholds $\{T_k^*\}$ satisfy

$$\sum_{j=1}^{K} B_j \Omega_{j\to k}^{\frac{\alpha_j-2}{\alpha_j}} \left(T_k^*\right)^{\frac{\alpha_j-2}{\alpha_j}} = D_l e^{\frac{\alpha_l-2}{2}C+\Theta_l-\tau_0},\ k\in\mathcal{K}, \tag{40}$$

where

$$\Omega_{j\to k} = \frac{P_{c,j}+\Delta_j p_j+P_{bh,j}}{P_{c,k}+\Delta_k p_k+P_{bh,k}},\ j,k\in\mathcal{K}. \tag{41}$$

Specially, when $\{\alpha_k\}=\alpha$, a closed-form expression of $\{T_k^*\}$ is given by

$$T_k^* = \left(\frac{\Xi e^{\frac{\alpha-2}{2}C-\tau_0}}{\sum_{j=1}^{K} B_j \Omega_{j\to k}^{\frac{\alpha-2}{\alpha}}} \right)^{\frac{\alpha}{\alpha-2}},\ k\in\mathcal{K}. \tag{42}$$

Proof: See Appendix D. ■

Note that the design of the optimal k^{th} RSS threshold jointly depends on multiple system parameters, including deployment density λ_k, transmit power p_k, circuit power $P_{c,k}$, backhaul power $P_{bh,k}$ and path loss exponent α_k. Particularly, T_k^* increases with the increment of $P_{c,k}$ and $P_{bh,k}$. This means that when the k^{th} tier has larger circuit power or backhaul power, the optimal cooperative region of the k^{th} tier will become smaller.

Furthermore, from (70) in Appendix D, the ratio of any two tiers' optimal RSS thresholds satisfies $\frac{T_j^*}{T_k^*} = \frac{P_{c,j}+\Delta_j p_j+P_{bh,j}}{P_{c,k}+\Delta_k p_k+P_{bh,k}},\ j,k\in\mathcal{K}$. That is, this ratio only depends on the power parameters of these two tiers. Accordingly, we can obtain insightful observations as follows.

[4]Note that there is no approximation in the process of solving the second sub-problem (39), and the optimal results in Theorem 3, which hold for all $k\in\mathcal{K}$ come from the combination of the above two sub-problems.

Remark 4: Since (40) is a polynomial equation, a simple binary search method or iterative method can be applied to compute the optimal result numerically. Meanwhile, due to the relationship between any two tiers' optimal RSS thresholds in (70), we just need to compute one nonlinear equation, which further reduces the computational complexity.

Remark 5: When the minimum spectral efficiency τ_0 increases, the most energy-efficient way to satisfy this rate requirement is to decrease each tier's RSS threshold T_k proportionally. On the contrary, adjusting only one tier's RSS threshold is always suboptimal in terms of energy saving, even if the power consumption per BS in this tier is low.

By substituting the optimal RSS thresholds in Theorem 3 into (6), the minimum area power consumption of the proposed clustering model can be obtained. In addition, to demonstrate the benefits of the proposed clustering model in terms of energy saving, in the following, we also derive the minimum area power consumption of the geometric clustering model in [23], [25] and [1]. In the geometric clustering model, the set of cooperative BSs from the k^{th} tier is defined as $\mathcal{C}_k = b(o,R_k)\cap\Phi_k$. Here, $b(o,R_k)$ denotes a two-dimensional ball centered at origin with a radius R_k. We call it a geometric scheme because the cooperative set of a typical user is only determined by the Euclidean distances between BSs and the typical user.

Taking computational complexity into account, however, we cannot allow the distribution of fading coefficients $\{\Psi_k\}$ to be arbitrary in this case. In order to effectively derive the optimal cooperative radii and keep the generality of the solution, we assume $\Psi_k \sim \Gamma(\nu_k,\mu_k)$ where $\Gamma(\nu_k,\mu_k)$ denotes Gamma distribution with shape ν_k and scale μ_k. Since it follows a similar derivation process, we directly give the result in the following proposition.

Proposition 3: Assume that fading coefficient $\Psi_k \sim \Gamma(\nu_k,\mu_k)$. In order to minimize the area power consumption while satisfying the minimum spectral efficiency requirement τ_0 under the geometric clustering model, the approximate value of the optimal K tiers' cooperative radii $\{R_k^*\}$ satisfy

$$\sum_{j=1}^{K} \tilde{B}_j \tilde{\Omega}_{j\to k}^{\frac{\alpha_j-2}{\alpha_j}} \left(R_k^*\right)^{\frac{\alpha_k(2-\alpha_j)}{\alpha_j}} = \tilde{D}_l e^{\frac{\alpha_l-2}{2}C+\tilde{\Theta}_l-\tau_0},\ k\in\mathcal{K}, \tag{43}$$

where $l\in\mathcal{K}$ and

$$\tilde{B}_k = \frac{(\alpha_K-2)\,p_k\nu_k\mu_k\lambda_k}{(\alpha_k-2)\,p_K\nu_K\mu_K\lambda_K},\ k\in\mathcal{K}, \tag{44}$$

$$\tilde{\Omega}_{j\to k} = \frac{\left(P_{c,j}+\Delta_j p_j+P_{bh,j}\right)p_k\nu_k\mu_k}{\left(P_{c,k}+\Delta_k p_k+P_{bh,k}\right)p_j\nu_j\mu_j},\ j,k\in\mathcal{K}, \tag{45}$$

$$\tilde{\Theta}_l = \int_0^\infty \frac{\exp\left(-\tilde{\omega}_l t^{\frac{2}{\alpha_l}}\right)}{t}\left[1-\exp\left(-\sum_{k=1,k\neq l}^{K}\tilde{\omega}_k t^{\frac{2}{\alpha_k}}\right)\right]dt, \tag{46}$$

$$\tilde{D}_l = \frac{\tilde{\omega}_l^{\frac{\alpha_l}{2}}}{\frac{2\pi}{\alpha_K-2}\lambda_K p_K \nu_K \mu_K}, \tag{47}$$

$$\tilde{\omega}_k = \pi\lambda_k(\mu_k p_k)^{\frac{2}{\alpha_k}}\varphi(\alpha_k,\nu_k),\ k\in\mathcal{K}, \tag{48}$$

TABLE I
SIMULATION PARAMETERS

Parameters	Value
Macro BS density (m^{-2}), λ_1	$1/\left(250^2\pi\right)$
Pico BS density (m^{-2}), λ_2	$1/\left(50^2\pi\right)$
User density (m^{-2}), λ_u	$1/\left(50^2\pi\right)$
Macro BS transmit powers (W), p_1	20
Pico BS transmit power (W), p_2	0.13
Macro BS circuit power (W), $P_{c,1}$	55
Pico BS circuit power (W), $P_{c,2}$	2.5
Macro BS non-transmission power (W), $P_{0,1}$	75
Pico BS non-transmission power (W), $P_{0,2}$	4.3
Slope of macro BS power consumption, Δ_1	4.7
Slope of pico BS power consumption, Δ_2	4
Macro tier path loss exponent, α_1	4.3
Pico tier path loss exponent, α_2	3.8
Standard deviation of macro tier fading (dB), ξ_1	6
Standard deviation of pico tier fading (dB), ξ_2	8

$$\varphi\left(\alpha_k, \nu_k\right) = \int_0^\infty \left(1 - \frac{1}{\left(1 + u^{-\frac{\alpha_k}{2}}\right)^{\nu_k}}\right) du. \quad (49)$$

By substituting the optimal cooperative radii $\{R_k^*\}$ into the area power consumption expression that $\tilde{P}_{area} = \sum_{k=1}^K \pi\lambda_u\lambda_k R_k^2\left(P_{c,k} + \Delta_k p_k + P_{bh,k}\right) + \sum_{k=1}^K \lambda_k P_{0,k}$, we can obtain the minimum area power consumption of the geometric clustering model. Note that under this Gamma distribution assumption, the value of $\mathbb{E}\left[\Psi_k^{2/\alpha_k}\right]$ in (28) can be evaluated as

$$\mathbb{E}\left[\Psi_k^{\frac{2}{\alpha_k}}\right] = \mu_k^{\frac{2}{\alpha_k}} \frac{\Gamma\left(\frac{2}{\alpha_k} + \nu_k\right)}{\Gamma\left(\nu_k\right)}. \quad (50)$$

As a result, the comparison of the proposed clustering model and the geometric model is presented in next section.

V. NUMERICAL RESULTS

In this section, we present the simulation results to validate our analysis and evaluate the energy saving performance under the proposed clustering model. Unless otherwise stated, we restrict our presented results to an interference-limited two-tier HetNet consisting of macro and pico BSs. Simulation parameters in the two-tier HetNet scenario are presented in Table I where the power parameters are chosen according to [39] and by default, the distribution of fading coefficient Ψ_k is assumed to be lognormal where $\Psi_k = 10^{\frac{x}{10}}$ with the Gauss random variable $x \sim N\left(0, \xi_k^2\right)$. In order to specify the value of $P_{bh,k}$, we consider a simplified backhaul system in [44]. According to expressions (3) and (5) of [44] by assuming that its weighting parameter $\alpha = 1$ and $max_{dl} = 30$, we obtain $P_{bh,1} = P_{bh,2} = 11$ W for our scenario[5].

In the Monte Carlo simulations, we choose a large spatial window, which is a square of 10 km $\times$ 10 km, and generate two independent PPPs of BS locations with their respective densities. For every realization, the fading coefficient $\Psi_{k,i}$ for each BS located at $x_{k,i}$ is independently generated according to $\Psi_{k,i} = 10^{\frac{x}{10}}$ with the Gauss random variable $x \sim N\left(0, \xi_k^2\right)$. Then the instantaneous user rate is obtained via (8) (by letting $\sigma^2 = 0$). The final simulation results are obtained by averaging 10000 independent realizations.

[5]Different from [44], here we only consider the downlink backhaul power, and thus $P_{bh,k}$ in (5) can be evaluated as $P_{bh,k} = P_{max}/max_{dl} + P_{dl}$ where P_{max} and P_{dl} are chosen according to TABLE II of [44].

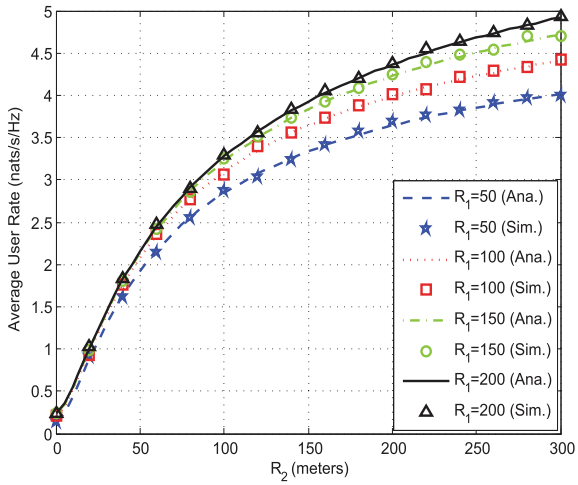

Fig. 2. Spectral efficiency as a function of mean cooperative radii, where R_1 and R_2 denote macro tier and pico tier mean cooperative radius, respectively.

A. Validation of Theorem 1

Fig. 2 shows the spectral efficiency of a typical user as a function of macro tier and pico tier mean cooperative radii. Note that since the mean cooperative radii $\{R_k\}$ and RSS thresholds $\{T_k\}$ are interchangeable according to (3), here we use $\{R_k\}$ as tunable parameters instead of $\{T_k\}$ for a better understanding. Compared with simulation results, the analytical integrations, i.e. Eq. (9) can be computed more efficiently and its accuracy is well verified by simulations. It can be seen that the spectral efficiency increases with both tiers' mean cooperative radii R_1 and R_2, since larger cooperative regions lead to higher useful signal strength and lower interference power. Besides, when the pico tier mean cooperative radius R_2 becomes sufficiently large, the increase of spectral efficiency becomes more marginal. This is because the average signal strength from the pico BSs in a long distance, in general, is weak, and the impact of those distant pico BSs on spectral efficiency can be neglected.

In order to elucidate the trade-off between the network power consumption and the spectral efficiency, we can consider the energy efficiency which can be effectively calculated according to (21). To this end, Fig. 3 shows the effect of macro tier and pico tier mean cooperative radii on the energy efficiency. It can be seen that for a fixed R_1, there exists an optimal value R_2^* which maximizes the energy efficiency; meanwhile, this optimal value R_2^* increases with R_1. This result gives us an insight in designing appropriate mean cooperative radii (or RSS thresholds) from the perspective of energy efficiency directly.

Furthermore, we can observe that energy efficiency increases as the macro tier mean cooperative radius decreases. This can be explained as follows: Compared with the positive impact on

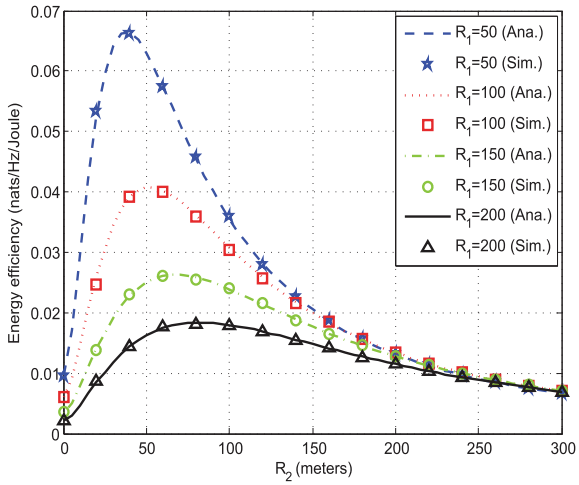

Fig. 3. Energy efficiency as a function of mean cooperative radii, where R_1 and R_2 denote macro tier and pico tier mean cooperative radius, respectively.

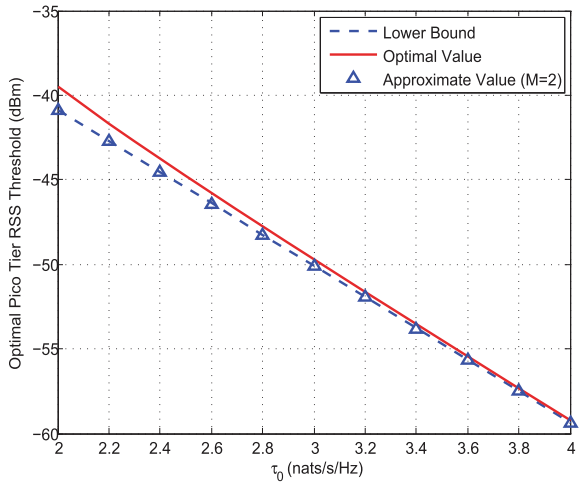

Fig. 4. The optimal pico tier RSS threshold as a function of minimum spectral efficiency τ_0 where $R_1 = 500$.

energy efficiency that more macro BSs will improve spectral efficiency, the negative impact on energy efficiency that more macro BSs will increase power consumption becomes more significant. In this figure, for example, $R_1 = 50$, $R_2 = 30$ is the best choice in terms of energy efficiency, but the spectral efficiency for the case of $R_1 = 50$, $R_2 = 30$ might be too small to satisfy the ever-increasing user rate requirement. Therefore, we should consider the tradeoff between spectral efficiency and energy efficiency in a practical scenario.

B. Tightness of Theorem 2

Note that we have developed the lower bound of the optimal K^{th} tier RSS threshold by fixing the first $K-1$ tiers' RSS thresholds in Theorem 2. It is important to see how tight the lower bound is. In the following, the lower bound is calculated directly according to Theorem 2 where Θ_2 $(l = 2)$ is calculated via (27). The optimal value is obtained from a binary search algorithm for (9). Also, since this is the case for $K = 2$ (i.e., a two-tier HetNet) and the parameter settings satisfy that $\omega_1 \omega_2^{-\frac{\alpha_2}{\alpha_1}} < 1$, a closed-form approximate value can be given by (33) where Θ_2 is calculated according to (32) with $M = 2$.

Fig. 4 shows the optimal pico tier RSS threshold as a function of minimum spectral efficiency, given a fixed value of the macro tier mean cooperative radius, i.e. $R_1 = 500$. First, it can be seen that the lower bound is close to the optimal value and their gap decreases as τ_0 increases. Since the value of τ_0 becomes increasingly large with the ever-increasing high traffic demand, this gap will be acceptable. Furthermore, we see that the approximate value is as accurate as the lower bound, which verifies the effectiveness of our approximation in the case of a two-tier HetNet. Namely, in a two-tier HetNet, we can effectively substitute the lower bound by the closed-form approximate value without losing accuracy.

Fig. 5 shows the optimal pico tier RSS threshold as a function of the macro tier mean cooperative radius, given a fixed value of minimum spectral efficiency, i.e. $\tau_0 = 4$. We can see that the gap between the lower bound and the optimal value is

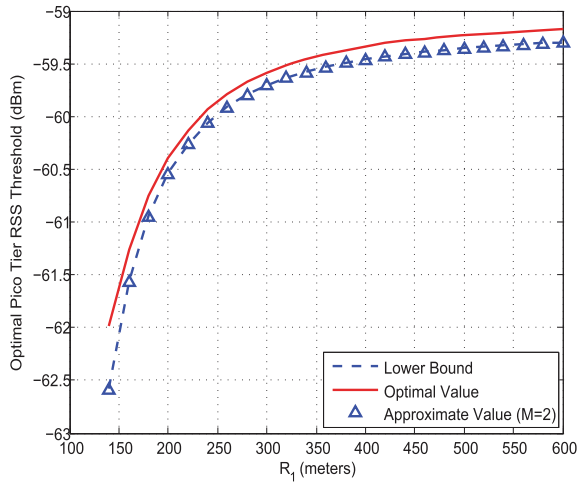

Fig. 5. The optimal pico tier RSS threshold as a function of the macro tier mean cooperative radius R_1 where $\tau_0 = 4$.

very small. When we have $R_1 = 300$, for instance, the gap is about 0.12 dB. More intuitively, if we consider the gap from the perspective of the optimal pico tier mean cooperative radius according to (3) equivalently, the gap is about 1.07 meters, which lies within the tolerable range. Therefore, the observations above verify the effectiveness of the lower bound. Besides, similar to Fig. 4, the approximate value also matches the lower bound perfectly, which further confirms the effectiveness of the closed-form approximation in a two-tier HetNet.

C. Area Power Consumption

Fig. 6 shows the minimum area power consumption under the proposed clustering model respectively in a traditional one-tier network, a two-tier HetNet consisting of macro and pico BSs and a three-tier HetNet consisting of macro, pico and femto BSs. The power parameters of femto BSs are also from [39], i.e. $p_3 = 0.05$, $P_{0,3} = 1.5$, $P_{c,3} = 3.3$, $\Delta_3 = 8$, and we also assume that the standard deviation of the femto tier fading coefficient is $\xi = 8$ dB. We observe that as the macro tier path loss

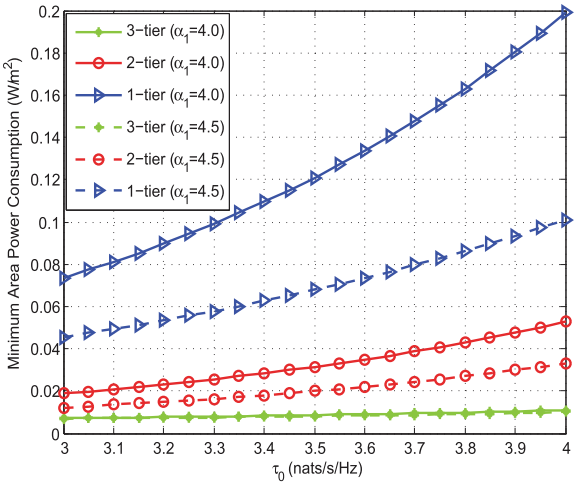

Fig. 6. The minimum area power consumption under the proposed clustering model respectively in a traditional one-tier network, a two-tier HetNet consisting of macro and pico BSs and a three-tier HetNet consisting of macro, pico and femto BSs where $\alpha_2 = 3.8, \alpha_3 = 3.5$.

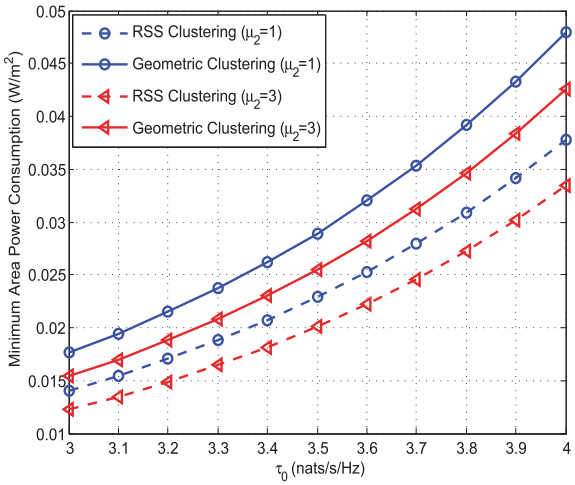

Fig. 7. The minimum area power consumption under the proposed clustering model vs. the geometric clustering model where fading coefficients satisfy $\Psi_{k,i} \sim \Gamma(\nu_k, \mu_k)$, $k = 1, 2$ and $\nu_1 = \nu_2 = 1, \mu_1 = 1$.

exponent α_1 increases, the area power consumption in all the cases decreases, and as the number of tiers increases, the impact of α_1 becomes increasingly marginal. This can be explained as follows: when the interference strength becomes smaller with the increment of macro tier path loss exponent, fewer cooperative BSs are needed to meet the minimum spectral efficiency requirement; in addition, when the number of tiers increases, fewer macro BSs will participate in cooperation.

More importantly, this figure shows that compared with the macro-only network, the extra deployment of pico and/or femto BSs is significantly more energy-saving. In particular, when we set the minimum average user rate to be 3.5 nats/s/Hz, the minimum area power consumption of a two-tier HetNet can be reduced by about 74.76% and 71.78% when $\alpha_1 = 4.0$ and $\alpha_1 = 4.5$, respectively. Note that the area power consumption will further decrease with the deployment of a three-tier HetNet. Therefore, it verifies the effectiveness of deploying the HetNets under the proposed clustering model from the perspective of energy saving.

Fig. 7 shows the minimum area power consumption varies with the minimum spectral efficiency τ_0, where we assume that the fading coefficient $\Psi_{k,i} \sim \Gamma(\nu_k, \mu_k)$. The curve "RSS Clustering" represents the proposed clustering model, and the curve "Geometric Clustering" represents geometric clustering model. It can be observed that when the channel gain increases or minimum spectral efficiency decreases, the minimum area power consumption decreases.

Furthermore, the minimum area power consumption of the proposed clustering model is less than that of the geometric clustering model. Particularly, when $\tau_0 = 3.5$ nats/s/Hz and $\mu_2 = 1$, applying the proposed clustering model can reduce by about 21% the minimum area power consumption. This result demonstrates the advantage of the proposed clustering model beyond the geometric policy. Intuitively, if the channel between a nearby BS and the typical user is in a deep shadow fading, information cannot be sent reliably over that link. Hence, this nearby BS will most probably not be considered as a serving BS. However, the geometric clustering model does not take the impact of shadow fading into account.

VI. Conclusions

In this paper, we considered BS cooperation in the downlink HetNets where BSs from different tiers within the respective cooperative clusters jointly transmit the same data to a typical user. A user-centric clustering model, based on tier-specific RSS threshold, was proposed. Then, we derived the spectral efficiency expression for a typical user located at the center of a cooperative cluster, from which we could also evaluate network throughput and energy efficiency. Furthermore, we formulated a power minimization problem with a minimum spectral efficiency constraint and derived its approximate solution which was shown to be highly accurate by simulations. Simulations showed that the proposed clustering model is more energy-saving compared to the geometric clustering model, and the extra deployment of small cells is significantly more energy-saving compared to the traditional macro-only network. Note that we have not considered the detailed selection procedure and its implementation complexity involved in the user-centric clustering model, and future work on this topic is still needed.

Appendix

A. Proof of Lemma 1

Without loss of generality, we consider a typical BS in the k^{th} tier which is located in x and denote by y_i the location of the i^{th} user, then $\mathcal{N}_k$ can be given by

$$\mathcal{N}_k = \sum_{y_i \in \Phi_u} 1\left\{p_k \Psi_{k,i} \|y_i - x\|^{-\alpha_k} \geq T_k\right\} \overset{(a)}{=} \sum_{y_{i,x} \in \Phi_{u,x}} 1\left\{p_k \Psi_{k,i} \|y_{i,x}\|^{-\alpha_k} \geq T_k\right\}, \quad (51)$$

where $1\{\cdot\}$ is an indicator function, (a) follows from a change of variable $y_{i,x} = y_i - x$, and $\Phi_{u,x} \overset{\Delta}{=} \Phi_u - x$. According to the

stationarity of the homogeneous PPP [43], the translated process $\Phi_{u,x}$ have the same distribution for all x in $\mathbb{R}^2$. Therefore, the mean value of $\mathcal{N}_k$ can be written as

$$\begin{aligned} L_k &= \mathbb{E}_{\Phi_{u,x},\Psi_{k,i}}\left[\sum_{y_{i,x}\in\Phi_{u,x}} 1\left\{p_k\Psi_{k,i}\left\|y_{i,x}\right\|^{-\alpha_k}\geq T_k\right\}\right] \\ &\overset{(a)}{=} \mathbb{E}_{\Psi_k}\left[2\pi\lambda_u\int_0^\infty 1\left\{p_k\Psi_k r^{-\alpha_k}\geq T_k\right\}rdr\right] \\ &= \pi\lambda_u\left(\frac{p_k}{T_k}\right)^{\frac{2}{\alpha_k}}\mathbb{E}\left[\Psi_k^{\frac{2}{\alpha_k}}\right], \end{aligned} \tag{52}$$

where (a) follows from the Campbell's theorem [43].

B. Proof of Theorem 2

From (18), we have

$$\begin{aligned} \mathcal{Z}(t,T_k,\alpha_k) &\leq \int_{(T_kt)^{-\frac{2}{\alpha_k}}}^\infty u^{-\frac{\alpha_k}{2}}du \\ &= \frac{2}{\alpha_k-2}(T_kt)^{\frac{\alpha_k-2}{\alpha_k}}, \end{aligned} \tag{53}$$

where the inequality follows from the fact that $1-e^{-x}\leq x, \forall x\geq 0$. Note that when T_k becomes smaller, the inequality in (53) becomes tighter.

Then by substituting (53) into (9) (letting $\sigma^2=0$), we can give an approximated lower bound of the spectral efficiency as

$$\begin{aligned} \tau \geq \int_0^\infty \frac{1}{t}\Bigg\{&\exp\left[-t\sum_{k=1}^K \pi\lambda_k\mathbb{E}\left[\Psi_k^{\frac{2}{\alpha_k}}\right]\frac{2}{\alpha_k-2}p_k^{\frac{2}{\alpha_k}}T_k^{\frac{\alpha_k-2}{\alpha_k}}\right] \\ &-\exp\left[-\sum_{k=1}^K \pi\lambda_k\mathbb{E}\left[\Psi_k^{\frac{2}{\alpha_k}}\right](tp_k)^{\frac{2}{\alpha_k}}\Gamma\left(1-\frac{\alpha_k}{2}\right)\right]\Bigg\}dt. \end{aligned} \tag{54}$$

Before deriving the lower bound of the optimal K^{th} RSS threshold, we first introduce the following lemma according to [45],

Lemma 2: Assume that $p>0, q>0$, then

$$\int_0^\infty \frac{1}{t}\left[\exp\left(-t^p\right)-\exp\left(-t^q\right)\right]dt = \frac{p-q}{pq}C, \tag{55}$$

where C is Euler's Constant.

By letting $\rho = \sum_{k=1}^K \pi\lambda_k\mathbb{E}\left[\Psi_k^{\frac{2}{\alpha_k}}\right]\frac{2}{\alpha_k-2}p_k^{\frac{2}{\alpha_k}}T_k^{\frac{\alpha_k-2}{\alpha_k}}$, (54) can be simplified as

$$\begin{aligned} \tau &\geq \int_0^\infty \frac{1}{t}\left[\exp(-\rho t)-\exp\left(-\sum_{k=1}^K\omega_k t^{\frac{2}{\alpha_k}}\right)\right]dt \\ &\overset{(a)}{=} \int_0^\infty \frac{1}{t}\left[\exp(-\rho t)-\exp\left(-\omega_l t^{\frac{2}{\alpha_l}}\right)\right]dt+\Theta_l \\ &\overset{(b)}{=} \int_0^\infty \frac{1}{y}\left[\exp(-y)-\exp\left(-\omega_l\rho^{-\frac{2}{\alpha_l}}y^{\frac{2}{\alpha_l}}\right)\right]dt+\Theta_l \\ &\overset{(c)}{=} \int_0^\infty \frac{1}{y}\left[\exp(-y)-\exp\left(-\omega_l^{\frac{\alpha_l}{2}}\rho^{-1}y\right)\right]dy \\ &\quad+\int_0^\infty \frac{1}{y}\left[\exp\left(-\omega_l^{\frac{\alpha_l}{2}}\rho^{-1}y\right)-\exp\left(-\omega_l\rho^{-\frac{2}{\alpha_l}}y^{\frac{2}{\alpha_l}}\right)\right]dy \\ &\quad+\Theta_l \\ &\overset{(d)}{=} \ln\left(\omega_l^{\frac{\alpha_l}{2}}\rho^{-1}\right)+\frac{\alpha_l-2}{2}C+\Theta_l, \end{aligned} \tag{56}$$

where $l\in\mathcal{K}$, (a) follows from the definition of Θ_l in (27) and (b) follows from a change of variable $y=\rho t$, (d) follows from (13) for evaluating the first integration in (c) and Lemma 2 for evaluating the second integration in (c). Finally, since the constraint is a strictly monotonically decreasing function of T_K, the optimization problem evolves into solving the equation that

$$\frac{\alpha_l-2}{2}C+\ln\left(\omega_l^{\frac{\alpha_l}{2}}\rho^{-1}\right)+\Theta_l=\tau_0. \tag{57}$$

By letting $T_K=T_K^d$, we have

$$\begin{aligned} \tau_0 =&\frac{\alpha_l-2}{2}C+\ln\omega_l^{\frac{\alpha_l}{2}}+\Theta_l \\ &-\ln\Bigg[\sum\nolimits_{k=1}^{K-1}\frac{2\pi}{\alpha_k-2}\lambda_k\mathbb{E}\left[\Psi_k^{\frac{2}{\alpha_k}}\right]p_k^{\frac{2}{\alpha_k}}T_k^{\frac{\alpha_k-2}{\alpha_k}} \\ &+\frac{2\pi}{\alpha_K-2}\lambda_K\mathbb{E}\left[\Psi_K^{\frac{2}{\alpha_K}}\right]p_K^{\frac{2}{\alpha_K}}\left(T_K^d\right)^{\frac{\alpha_K-2}{\alpha_K}}\Bigg]. \end{aligned} \tag{58}$$

Solving (58) gives the expression of the lower bound T_K^d.

C. Proof of Proposition 2

Let $y=\left(T_K^d\right)^{\frac{\alpha-2}{\alpha}}$, then from (35), we have

$$y=\delta\frac{\left(\sum_{k=1}^K\omega_k\right)^{\frac{\alpha}{2}}}{\omega_K}-\sum_{k=1}^{K-1}\frac{\omega_kT_k^{\frac{\alpha-2}{\alpha}}}{\omega_K}, \tag{59}$$

where $\delta\triangleq\left(\frac{\alpha}{2}-1\right)\Gamma\left(1-\frac{2}{\alpha}\right)e^{\frac{\alpha-2}{2}C-\tau_0}$ and

$$\omega_k=\pi\lambda_k\mathbb{E}\left[\Psi_k^{\frac{2}{\alpha}}\right]p_k^{\frac{2}{\alpha}}\Gamma\left(1-\frac{2}{\alpha}\right),\ k\in\mathcal{K}. \tag{60}$$

Taking the derivative with respect to y (ω_K) results in

$$\begin{aligned} \frac{\partial y(\omega_K)}{\partial\omega_K} = \frac{1}{\omega_K^2}\Bigg[&\delta\left(\sum_{k=1}^K\omega_k\right)^{\frac{\alpha}{2}-1}\left(\frac{\alpha-2}{2}\omega_K-\sum_{k=1}^{K-1}\omega_k\right) \\ &+\sum_{k=1}^{K-1}\omega_kT_k^{\frac{\alpha-2}{\alpha}}\Bigg]. \end{aligned} \tag{61}$$

First, note that $\frac{\partial y(\omega_K)}{\partial\omega_K}\geq 0$ when

$$\frac{\alpha-2}{2}\omega_K-\sum\nolimits_{k=1}^{K-1}\omega_k\geq 0. \tag{62}$$

Since T_K^d is a strictly monotonically increasing function of y and ω_K is an affine function of λ_K, T_K^d increases with λ_K

when λ_K satisfies the inequality (62). Second, when $\frac{\alpha-2}{2}\omega_K - \sum_{k=1}^{K-1}\omega_k < 0$, from (61), we have

$$\begin{aligned}\frac{\partial y(\omega_K)}{\partial \omega_K} \leq & \frac{1}{\omega_K^2}\left[\delta\left(\sum_{k=1}^{K}\omega_{K-1}\right)^{\frac{\alpha}{2}-1}\left(\frac{\alpha-2}{2}\omega_K - \sum_{k=1}^{K-1}\omega_k\right)\right. \\ & \left. + \sum_{k=1}^{K-1}\omega_k T_k^{\frac{\alpha-2}{\alpha}}\right] \\ \triangleq & h(\omega_K). \end{aligned} \tag{63}$$

Therefore, $\frac{\partial y(\omega_K)}{\partial \omega_K} \leq 0$ when

$$h(\omega_K) \leq 0. \tag{64}$$

Similarly, we can conclude that T_K^d decreases with λ_K when λ_K satisfies the inequality (64).

Finally, by substituting (60) into (62) and (64), we can get $\mathcal{G}_1$ and $\mathcal{G}_2$, respectively.

D. Proof of Theorem 3

First, we assume that $\tilde{f}(\mathbb{T}_{-K})$ is a function defined on

$$\mathcal{E} = \left\{ \mathbb{T}_{-K} \left| D_l e^{\frac{\alpha_l-2}{2}C+\Theta_l-\tau_0} - \sum_{k=1}^{K-1} B_k T_k^{\frac{\alpha_k-2}{\alpha_k}} \geq 0, T_k \geq 0 \right.\right\} \tag{65}$$

and satisfies that

$$\begin{aligned}\tilde{f}(\mathbb{T}_{-K}) = & \sum_{k=1}^{K-1} B_k \frac{\alpha_k-2}{\alpha_K-2}\Omega_{k\to K} T_k^{\frac{2}{\alpha_k}} \\ & + \left(D_l e^{\frac{\alpha_l-2}{2}C+\Theta_l-\tau_0} - \sum_{k=1}^{K-1} B_k T_k^{\frac{\alpha_k-2}{\alpha_k}}\right)^{\frac{2}{2-\alpha_K}}. \end{aligned} \tag{66}$$

Thus the problem (39) can be transformed as

$$\mathbb{T}_{-K}^* = \arg\min_{\mathbb{T}_{-K}} \tilde{f}(\mathbb{T}_{-K}), \tag{67}$$

where $\mathbb{T}_{-K}^* = \left[T_1^*, T_2^*, \cdots, T_{K-1}^*\right]$.

By setting its derivative over T_k to 0, i.e. $\frac{\partial \tilde{f}(\mathbb{T}_{-K})}{\partial T_k} = 0$, equivalently we have

$$\begin{aligned} & B_k \frac{\alpha_k-2}{\alpha_K-2}\Omega_{k\to K}\left(-\frac{2}{\alpha_k}\right)T_k^{-\frac{2}{\alpha_k}-1} - \frac{2}{2-\alpha_K} \\ & \cdot\left(D_l e^{\frac{\alpha_l-2}{2}C+\Theta_l-\tau_0} - \sum_{k=1}^{K-1} B_k T_k^{\frac{\alpha_k-2}{\alpha_k}}\right)^{\frac{\alpha_K}{2-\alpha_K}} \frac{\alpha_k-2}{\alpha_k} B_k T_k^{-\frac{2}{\alpha_k}} \\ & = 0, \quad k = 1, 2, \cdots, K-1. \end{aligned} \tag{68}$$

Solving the above equation, we have

$$T_k^* = \Omega_{k\to K}\left(D_l e^{\frac{\alpha_l-2}{2}C+\Theta_l-\tau_0} - \sum_{j=1}^{K-1} B_j\left(T_j^*\right)^{\frac{\alpha_j-2}{\alpha_j}}\right)^{\frac{\alpha_K}{\alpha_K-2}}, \tag{69}$$

where $k = 1, 2, \cdots, K-1$. Considering the relationship of T_k^* and T_j^*, we have

$$T_j^* = \Omega_{j\to k} T_k^*, \quad k, j = 1, 2, \cdots, K-1. \tag{70}$$

Substituting (70) into (69), the result is given as

$$\sum_{j=1}^{K} B_j \Omega_{j\to k}^{\frac{\alpha_j-2}{\alpha_j}}\left(T_k^*\right)^{\frac{\alpha_j-2}{\alpha_j}} = D_l e^{\frac{\alpha_l-2}{2}C+\Theta_l-\tau_0}, \tag{71}$$

where $k = 1, 2, \cdots, K-1$. According to the result of (69), the optimal values $\mathbb{T}_{-K}^*$ satisfy that

$$\begin{aligned} D_l e^{\frac{\alpha_l-2}{2}C+\Theta_l-\tau_0} - \sum_{j=1}^{K-1} B_j\left(T_j^*\right)^{\frac{\alpha_j-2}{\alpha_j}} &= \left(T_k^*\right)^{\frac{\alpha_K-2}{\alpha_K}}\Omega_{K\to k} \\ &\geq 0, \end{aligned} \tag{72}$$

which means $\mathbb{T}_{-K}^* \in \mathcal{E}$. According to [46], since $\tilde{f}(\mathbb{T}_{-K})$ is a convex function at its domain of definition $\mathcal{E}$, the optimal value $\mathbb{T}_{-K}^*$ in (71) is the solution of problem (39).

Furthermore, by letting $k = K$ in (71), we have

$$\begin{aligned} \sum_{j=1}^{K} B_j \Omega_{j\to K}^{\frac{\alpha_j-2}{\alpha_j}}\left(T_K^*\right)^{\frac{\alpha_j-2}{\alpha_j}} &= \sum_{j=1}^{K-1} B_j \Omega_{j\to K}^{\frac{\alpha_j-2}{\alpha_j}}\left(T_K^*\right)^{\frac{\alpha_j-2}{\alpha_j}} + \left(T_K^*\right)^{\frac{\alpha_K-2}{\alpha_K}} \\ &\overset{(a)}{=} D_l e^{\frac{\alpha_l-2}{2}C+\Theta_l-\tau_0}, \end{aligned} \tag{73}$$

where (a) follows from (24) in Theorem 2, then (71) holds for all $k \in \mathcal{K}$ and thus serves as an optimal solution of the original problem (22).

Acknowledgment

The authors wish to thank the anonymous reviewers for their constructive comments.

References

[1] W. Nie, X. Wang, F. Zheng, and W. Zhang, "Energy-efficient base station cooperation in downlink heterogeneous cellular networks," in *Proc. IEEE Global Telecommun. Conf. (Globecom)*, Dec. 2014, pp. 1779–1784.

[2] G. P. Fettweis and E. Zimmermann, "ICT energy consumption-trends and challenges," in *Proc. 11th Int. Symp. Wireless Pers. Multimedia Commun. (WPMC)*, Sep. 2008, p. 6.

[3] Telecommunication management; Study on Energy Savings Management (ESM), (Release 10)," 3GPP TR 32.826, Mar. 2010 [Online]. Available: http://www.3gpp.org/ftp/Specs/html-info/32826.htm

[4] L. M. Correia *et al.*, "Challenges and enabling technologies for energy aware mobile radio networks," *IEEE Commun. Mag.*, vol. 48, no. 11, pp. 66–72, Nov. 2010.

[5] X. Wang, A. V. Vasilakos, M. Chen, Y. Liu, and T. T. Kwon, "A survey of green mobile networks: Opportunities and challenges," *J. Mobile Netw. Appl.*, vol. 17, no. 1, pp. 4–20, Feb. 2012.

[6] Z. Hasan, H. Boostanimehr, and V. K. Bhargava, "Green cellular networks: A survey, some research issues and challenges," *IEEE Commun. Surv. Tuts.*, vol. 13, no. 4, pp. 524–540, Fourth Quart. 2011.

[7] T. Q. S. Quek, G. de la Roche, I. Guvenc, and M. Kountouris, *Small Cell Networks: Deployment, PHY Techniques, and Resource AllocaBon*. Cambridge, U.K.: Cambridge Univ. Press, 2013.

[8] Qualcomm, "LTE advanced: Heterogeneous networks," White Paper, Jan. 2011.

[9] D. Lopez-Perez, I. Guvenc, G. de la Roche, M. Kountouris, T. Q. S. Quek, and J. Zhang, "Enhanced intercell interference coordination challenges in heterogeneous networks," *IEEE Wireless Commun. Mag.*, vol. 18, no. 3, pp. 22–30, Jun. 2011.

[10] 3GPP TR 36.819, "Coordinated multi-point operation for LTE physical layer aspects (Release 11)," 3GPP, Sophia Antipolis, France, Tech. Rep., Sep. 2011, v11.1.0.
[11] D. Gesbert, S. Hanly, H. Huang, S. Shamai, O. Simeone, and W. Yu, "Multi-cell MIMO cooperative networks: A new look at interference," *IEEE J. Sel. Areas Commun.*, vol. 28, no. 9, pp. 1380–1408, Dec. 2010.
[12] H. Dahrouj and W. Yu, "Coordinated beamforming for the multicell multiantenna wireless system," *IEEE Trans. Wireless Commun.*, vol. 9, no. 5, pp. 1748–1759, May 2010.
[13] M. Sawahashi, Y. Kishiyama, A. Morimoto, D. Nishikawa, and M. Tanno, "Coordinated multipoint transmission/reception techniques for LTE-advanced [coordinated and distributed MIMO]," *IEEE Wireless Commun. Mag.*, vol. 17, no. 3, pp. 26–34, Jun. 2010.
[14] A. Lozano, R. W. Heath, and J. G. Andrews, "Fundamental limits of cooperation," *IEEE Trans. Inf. Theory*, vol. 59, no. 9, pp. 5213–5226, Sep. 2013.
[15] F. Boccardi, R. W. Heath, A. Lozano, T. L. Marzetta, and P. Popovski, "Five disruptive technology directions for 5G," *IEEE Commun. Mag.*, vol. 52, no. 2, pp. 74–80, Feb. 2014.
[16] M. Haenggi, J. G. Andrews, F. Baccelli, O. Dousse, and M. Franceschetti, "Stochastic geometry and random graphs for the analysis and design of wireless networks," *IEEE J. Sel. Areas Commun.*, vol. 27, no. 7, pp. 1029–1046, Sep. 2009.
[17] J. G. Andrews, F. Baccelli, and R. K. Ganti, "A tractable approach to coverage and rate in cellular networks," *IEEE Trans. Commun.*, vol. 59, no. 11, pp. 3122–3134, Nov. 2011.
[18] H. S. Dhillon, R. K. Ganti, F. Baccelli, and J. G. Andrews, "Modeling and analysis of K-tier downlink heterogeneous cellular networks," *IEEE J. Sel. Areas Commun.*, vol. 30, no. 3, pp. 550–560, Apr. 2012.
[19] H.-S. Jo, Y. J. Sang, P. Xia, and J. G. Andrews, "Heterogeneous cellular networks with flexible cell association: A comprehensive downlink SINR analysis," *IEEE Trans. Wireless Commun.*, vol. 11, no. 10, pp. 3484–3495, Oct. 2012.
[20] K. Huang and J. G. Andrews, "An analytical framework for multicell cooperation via stochastic geometry and large deviations," *IEEE Trans. Inf. Theory*, vol. 59, no. 4, pp. 2501–2516, Apr. 2013.
[21] S. Akoum and R. W. Heath, "Interference coordination: Random clustering and adaptive limited feedback," *IEEE Trans. Signal Process.*, vol. 61, no. 7, pp. 1822–1834, Apr. 2013.
[22] F. Baccelli and A. Giovanidis, "A stochastic geometry framework for analyzing pairwise-cooperative cellular networks," *IEEE Trans. Wireless Commun.*, vol. 14, no. 2, pp. 794–808, Feb. 2015.
[23] R. Tanbourgi, S. Singh, J. G. Andrews, and F. K. Jondral, "A tractable model for non-coherent joint-transmission base station cooperation," *IEEE Trans. Wireless Commun.*, vol. 13, no. 9, pp. 4959–4973, Sep. 2014.
[24] Y. Lin and W. Yu, "Ergodic capacity analysis of downlink distributed antenna systems using stochastic geometry," in *Proc. IEEE Int. Conf. Commun. (ICC)*, Jun. 2013, pp. 3338–3343.
[25] R. Tanbourgi, S. Singh, J. G. Andrews, and F. K. Jondral, "Analysis of non-coherent joint-transmission cooperation in heterogeneous cellular networks," in *Proc. IEEE Int. Conf. Commun. (ICC)*, Jun. 2014, pp. 5160–5165.
[26] G. Nigam, P. Minero, and M. Haenggi, "Coordinated multipoint joint transmission in heterogeneous networks," *IEEE Trans. Commun.*, vol. 62, no. 11, pp. 4134–4146, Nov. 2014.
[27] Z. Xu, C. Yang, G. Y. Li, Y. Liu, and S. Xu, "Energy-efficient CoMP precoding in heterogeneous networks," *IEEE Trans. Signal Process.*, vol. 62, no. 4, pp. 1005–1017, Feb. 2014.
[28] S. He, Y. Huang, H. Wang, S. Jin, and L. Yang, "Leakage-aware energy-efficient beamforming for heterogeneous multicell multiuser systems," *IEEE J. Sel. Areas Commun.*, vol. 32, no. 6, pp. 1268–1281, Jun. 2014.
[29] J. Tang, D. So, E. Alsusa, K. A. Hamdi, and A. Shojaeifard, "Resource allocation for energy efficiency optimization in heterogeneous networks," *IEEE J. Sel. Areas Commun.*, vol. 33, no. 10, pp. 2104–2117, Oct. 2015.
[30] T. Quek, W. Cheung, and K. Marios, "Energy efficiency analysis of two-tier heterogeneous networks," in *Proc. 11th Eur. Wireless Conf.—Sustain. Wireless Technol.*, Apr. 2011, pp. 1–5.
[31] Y. S. Soh, T. Q. S. Quek, M. Kountouris, and H. Shin, "Energy efficient heterogeneous cellular networks," *IEEE J. Sel. Areas Commun.*, vol. 31, no. 5, pp. 840–850, May 2013.
[32] Z. Wang and W. Zhang, "A separation architecture for achieving energy-efficient cellular networking," *IEEE Trans. Wireless Commun.*, vol. 13, no. 6, pp. 3113–3123, Jun. 2014.
[33] Y. Huang *et al.*, "Energy-efficient design in heterogeneous cellular networks based on large-scale user behavior constraints," *IEEE Trans. Wireless Commun.*, vol. 13, no. 9, pp. 4746–4757, Sep. 2014.
[34] H. ElSawy and E. Hossain, "Two-tier HetNets with cognitive femtocells: Downlink performance modeling and analysis in a multichannel environment," *IEEE Trans. Mobile Comput.*, vol. 13, no. 3, pp. 649–663, Mar. 2014.
[35] Ericsson, "Discussions on DL CoMP schemes," 3rd Generation Partnership Project (3GPP), Sophia-Antipolis, France, Tech. Rep. 3GPP TSG-RAN WG1#66 R1–113353, Oct. 2011.
[36] J. Andrews, "Seven ways that HetNets are a cellular paradigm shift," *IEEE Commmun. Mag.*, vol. 51, no. 3, pp. 136–144, Mar. 2013.
[37] T. R. Lakshmana, B. Makki, and T. Svensson, "Frequency allocation in non-coherent joint transmission CoMP networks," in *Proc. IEEE Int. Conf. Commun. (ICC) Workshops*, Jun. 2014, pp. 610–615.
[38] B. Blaszczyszyn, M. K. Karray, and H. P. Keeler, "Using Poisson processes to model lattice cellular networks," in *Proc. IEEE INFOCOM*, Apr. 2013, pp. 773–781.
[39] G. Auer *et al.*, "How much energy is needed to run a wireless network?," *IEEE Wireless Commun. Mag.*, vol. 18, no. 5, pp. 40–49, Oct. 2011.
[40] G. Auer *et al.*, "D2.3: Energy efficiency analysis of the reference systems, areas of improvements and target breakdown," EARTH (Energy Aware Radio and neTwork tecHnologies), EU Funded Research Project FP7-ICT-2009-4-247733-EARTH, Nov. 2010 [Online]. Available: https://www.ict-earth.eu
[41] A. J. Fehske, P. Marsch, and G. P. Fettweis, "Bit per Joule efficiency of cooperating base stations in cellular networks," in *Proc. IEEE Global Telecommun. Conf. (Globecom) Workshops*, Dec. 2010, pp. 1406–1411.
[42] K. Hamdi, "Capacity of MRC on correlated Rician fading channels," *IEEE Trans. Commun.*, vol. 56, no. 5, pp. 708–711, May 2008.
[43] S. N. Chiu, D. Stoyan, W. S. Kendall, and J. Mecke, *Stochastic Geometry and Its Applications*, 3rd ed. Hoboken, NJ, USA: Wiley, 2013.
[44] S. Tombaz, P. Monti, K. Wang, A. Vastberg, M. Forzati, and J. Zander, "Impact of backhauling power consumption on the deployment of heterogeneous mobile networks," in *Proc. IEEE Global Telecommun. Conf. (Globecom)*, Dec. 2011, pp. 1–5.
[45] A. Jeffrey and D. Zwillinger, *Table of Integrals, Series, and Products*. New York, NY, USA: Academic, 2007.
[46] S. Boyd and L. Vandenberghe, *Convex Optimization*. Cambridge, U.K.: Cambridge Univ. Press, 2004.

Weili Nie received the B.S. degree in electronics and information engineering from Huazhong University of Science and Technology, China, in 2012, and the M.S. degree in electrical engineering from Southeast University, China, in 2015. His research interests include wireless networks, green communications and statistical signal processing.

Fu-Chun Zheng (M'95–SM'99) received the B.Eng. and M.Eng. degrees in radio engineering from Harbin Institute of Technology, China, in 1985 and 1988, respectively, and the Ph.D. degree in electrical engineering from the University of Edinburgh, Edinburgh, U.K., in 1992.

From 1992 to 1995, he was a Postdoctoral Research Associate with the University of Bradford, Bradford, U.K. Between May 1995 and August 2007, he was with Victoria University, Melbourne, Vic., Australia, first as a Lecturer and then as an Associate Professor of mobile communications. He joined the University of Reading, Reading, U.K., in September 2007, as Professor (Chair) of signal processing. He has received two U.K. EPSRC Visiting Fellowships—both hosted by the University of York, York, U.K.: first from August 2002 to July 2003 and then from August 2006 to July 2007. Over the past 20 years, he has also carried out many government and industry sponsored research projects and authored more than 140 refereed journal and conference papers. He has been both a short-term Visiting Fellow and a long-term Visiting Research Fellow with British Telecom, U.K. His research interests include signal processing for communications, multiple antenna systems, and green communications.

He was an Editor (2001–2004) of the IEEE TRANSACTIONS ON WIRELESS COMMUNICATIONS. In 2006, he served as the General Chair of the IEEE VTC 2006-Spring in Melbourne, Vic., Australia—the first ever VTC held in the southern hemisphere in VTC's history of six decades. He is the Co-Ordinator and a Lead TPC Co-Chair for VTC 2016-S in Nanjing, China (the first VTC in mainland China.

Xiaoming Wang received the M.S. degree in communication and information system from Shandong University of Science and Technology, Qingdao, China, in 2011. He is currently pursuing the Ph.D degree at the National Mobile Communications Research Laboratory (NCRL), Southeast University, Nanjing, China. His research interests include communication and signal processing, including green communication systems, resource allocation and cooperative communication.

Wenyi Zhang (S'00–M'07–SM'11) received the bachelor's degree in automation from Tsinghua University, in 2001, and the master's and Ph.D. degrees, both in electrical engineering, from the University of Notre Dame, IN, USA, in 2003 and 2006, respectively. He is a Faculty member with the Department of Electronic Engineering and Information Science, University of Science and Technology of China, Hefei, China. Prior to that, he was affiliated with the Communication Science Institute, University of Southern California, as a Postdoctoral Research Associate, and with Qualcomm Incorporated, Corporate Research and Development. His research interests include wireless communications and networking, information theory, and statistical signal processing.

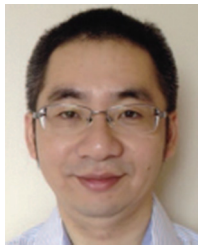

Shi Jin (S'06–M'07) received the B.S. degree in communications engineering from Guilin University of Electronic Technology, Guilin, China, in 1996, the M.S. degree from Nanjing University of Posts and Telecommunications, Nanjing, China, in 2003, and the Ph.D. degree in communications and information systems from the Southeast University, Nanjing, China, in 2007. From June 2007 to October 2009, he was a Research Fellow with the Adastral Park Research Campus, University College London, London, U.K. He is currently a Faculty member with the National Mobile Communications Research Laboratory, Southeast University. His research interests include space time wireless communications, random matrix theory, and information theory. He serves as an Associate Editor for the IEEE TRANSACTIONS ON WIRELESS COMMUNICATIONS, IEEE COMMUNICATIONS LETTERS, and *IET Communications*. He and his coauthors were the recipients of the 2011 IEEE Communications Society Stephen O. Rice Prize Paper Award in the field of communication theory and a 2010 Young Author Best Paper Award by the IEEE Signal Processing Society.